

This is a repository copy of *Pulse pile-up identification and reconstruction for liquid scintillator based neutron detectors*.

White Rose Research Online URL for this paper:  
<https://eprints.whiterose.ac.uk/132689/>

Version: Accepted Version

---

**Article:**

Luo, X. L., Modamio, V., Nyberg, J. et al. (20 more authors) (2018) Pulse pile-up identification and reconstruction for liquid scintillator based neutron detectors. *Nuclear Instruments and Methods in Physics Research, Section A: Accelerators, Spectrometers, Detectors and Associated Equipment*. pp. 59-65. ISSN 0168-9002

<https://doi.org/10.1016/j.nima.2018.03.078>

---

**Reuse**

This article is distributed under the terms of the Creative Commons Attribution-NonCommercial-NoDerivs (CC BY-NC-ND) licence. This licence only allows you to download this work and share it with others as long as you credit the authors, but you can't change the article in any way or use it commercially. More information and the full terms of the licence here: <https://creativecommons.org/licenses/>

**Takedown**

If you consider content in White Rose Research Online to be in breach of UK law, please notify us by emailing [eprints@whiterose.ac.uk](mailto:eprints@whiterose.ac.uk) including the URL of the record and the reason for the withdrawal request.

# 1 Pulse pile-up identification and reconstruction for liquid scintillator 2 based neutron detectors

3

4 X.L. Luo<sup>a,b</sup>, V. Modamio<sup>c</sup>, J. Nyberg<sup>b</sup>, J.J. Valiente-Dobón<sup>c</sup>, Q. Nishada<sup>b</sup>, G. de Angelis<sup>c</sup>,  
5 J. Agramunt<sup>d</sup>, F.J. Egea<sup>d,e</sup>, M.N. Erduran<sup>f</sup>, S. Ertürk<sup>g</sup>, G. de France<sup>h</sup>, A. Gadea<sup>d</sup>, V. González<sup>e</sup>,  
6 A. Goasduff<sup>i</sup>, T. Hüyük<sup>d</sup>, G. Jaworski<sup>j,k</sup>, M. Moszyński<sup>k,l</sup>, A. Di Nitto<sup>m</sup>, M. Palacz<sup>k</sup>, P.-A.  
7 Söderström<sup>n,o</sup>, E. Sanchis<sup>c</sup>, A. Triossi<sup>c</sup>, R. Wadsworth<sup>p</sup>

8

9 <sup>a</sup> National Innovation Institute of Defense Technology, Academy of Military Sciences, Beijing 100010, China

10 <sup>b</sup> Department of Physics and Astronomy, Uppsala University, SE-75120 Uppsala, Sweden

11 <sup>c</sup> INFN, Laboratori Nazionali di Legnaro, I-35020 Legnaro (Padova), Italy

12 <sup>d</sup> IFIC-CSIC, University of Valencia, Valencia, Spain

13 <sup>e</sup> Department of Electronic Engineering, University of Valencia, E-46071 Valencia, Spain

14 <sup>f</sup> Faculty of Engineering and Natural Sciences, Istanbul Sabahattin Zaim University Istanbul, Turkey

15 <sup>g</sup> Omer Halisdemir University, Nigde, Turkey

16 <sup>h</sup> GANIL, CEA/DSAM and CNRS/IN2P3, Bd Henri Becquerel, BP 55027, F-14076 Caen Cedex 05, France

17 <sup>i</sup> Dipartimento di Fisica e Astronomia, Università di Padova, Padova, Italy

18 <sup>j</sup> Faculty of Physics, Warsaw University of Technology, ul. Koszykowa 75, 00-662 Warszawa, Poland

19 <sup>k</sup> Heavy Ion Laboratory, University of Warsaw, ul. Pasteura 5A, 02-093 Warszawa, Poland

20 <sup>l</sup> National Centre for Nuclear Research, A. Soltana 7, PL 05-400 Otwock-Swierk, Poland

21 <sup>m</sup> Johannes Gutenberg-Universität Mainz, 55099 Mainz, Germany

22 <sup>n</sup> Institut für Kernphysik, TU Darmstadt, D-64289 Darmstadt, Germany

23 <sup>o</sup> GSI Helmholtzzentrum für Schwerionenforschung GmbH, 64291 Darmstadt, Germany

24 <sup>p</sup> Department of Physics, University of York, Heslington, York, YO10 5DD, UK

25

26 **Abstract:** The issue of pulse pile-up is frequently encountered in nuclear experiments involving  
27 high counting rates, which will distort the pulse shapes and the energy spectra. A digital method of  
28 off-line processing of pile-up pulses is presented. The pile-up pulses were firstly identified by detecting  
29 the downward-going zero-crossings in the first-order derivative of the original signal, and then the  
30 constituent pulses were reconstructed based on comparing the pile-up pulse with four models that are  
31 generated by combining pairs of neutron and  $\gamma$  standard pulses together with a controllable time  
32 interval. The accuracy of this method in resolving the pile-up events was investigated as a function of  
33 the time interval between two pulses constituting a pile-up event. The obtained results show that the  
34 method is capable of disentangling two pulses with a time interval among them down to 20 ns, as well  
35 as classifying them as neutrons or  $\gamma$  rays. Furthermore, the error of reconstructing pile-up pulses could  
36 be kept below 6% when successive peaks were separated by more than 50 ns. By applying the method  
37 in a high counting rate of pile-up events measurement of the NEutron Detector Array (NEDA), it was  
38 empirically found that this method can reconstruct the pile-up pulses and perform neutron- $\gamma$   
39 discrimination quite accurately. It can also significantly correct the distorted pulse height spectrum due  
40 to pile-up events.

41

42 **Keywords:** pile-up; digital; first-order derivative; neutron- $\gamma$  discrimination; liquid scintillator.

## 43 **1. Introduction**

44 High counting rates in radiation detectors is a common fact in nuclear  
45 spectroscopy as well as in nuclear reaction studies. For such applications involving  
46 high counting rates, the pile-up effect, in which more than one event occur  
47 simultaneously or closely spaced in time, becomes a severe issue. It results in two or  
48 more recorded signals partially or even completely overlapping, thus leading to a  
49 decrease in the counting efficiency, distortion of the pulse shape, and deterioration in  
50 the energy resolution.

51 Typically, pile-up events are diminished by reducing the pulse width with  
52 shaping networks, at the expense of a poorer performance in terms of  
53 signal-to-noise ratio. Since compressing signal pulses can only reduce the probability  
54 of the occurrence of pile-up but cannot totally eliminate it, hardware-based pile-up  
55 rejectors are often employed to identify the inevitable pile-up events and then discard  
56 them [1-4]. Although rejectors of this type can reduce the spectral distortions arising  
57 from pile-up to some extent, they negatively impact on the system throughput.  
58 Furthermore, some recorded events correspond to the pile-up of pulses that almost  
59 completely overlap, so that the recorded amplitude distribution is still distorted  
60 compared with the true event spectrum.

61 With the availability of digital signal processing techniques, digital treatments of  
62 pile-up have been introduced and adopted which yield significant advantages over  
63 conventional analog approaches. However, these are typically quite complex and not  
64 yet routinely employed in standard spectroscopy systems in which the pulse analysis  
65 is carried out in real time. The digital methods offer the possibility of preserving and  
66 analyzing in detail all the information carried by the overlapping pulses rather than  
67 simply rejecting them and tolerating the losses due to pile-up [5]. Various developed  
68 algorithms, such as the fitting method [6,7] and the deconvolution method [8], have  
69 successfully disentangled pile-up pulses with good accuracy, provided that a  
70 minimum time interval of around 40-50 ns exists between the two successive pulses  
71 constituting a pile-up event. Not only these methods compensate for the counting  
72 losses and correct the spectral distortions resulting from pile-up, but they are also  
73 capable of recovering original information on the type and energy of the constituent  
74 particles of the pile-up events. However, most of the methods are somewhat limited  
75 by analytical and computational complexity. For instance, the fitting process of the  
76 pulse based on an exponential analytic model has to be performed by trial and error,  
77 as sometimes it is hard for the fitting to converge to the correct solution. In this study,  
78 the aim is to propose an easy-implemented and efficient method of pulse pile-up  
79 identification and reconstruction for signals from liquid scintillators similar to the  
80 type that are used by the neutron detector array NEDA [9-12]. The ongoing NEDA  
81 project addresses the physics of neutron-deficient as well as neutron-rich nuclei using  
82 both intense stable and radioactive ion beams. The full version of NEDA will consist  
83 of around 350 closely packed liquid scintillator detectors of type BC-501A, mainly in  
84 conjunction with large  $\gamma$ -ray arrays like AGATA [13,14]. For use in nuclear structure  
85 experiments, NEDA should have the capability to run at high counting rates, which

86 leads to a significant fraction of pile-up events, while retaining a high neutron  
87 efficiency and an excellent neutron-gamma ( $n\text{-}\gamma$ ) discrimination performance. In order  
88 to meet these requirements, the pile-up issue has to be dealt with appropriately in  
89 NEDA. Specifically, the idea is to identify pile-up pulses and then perform  $n\text{-}\gamma$   
90 discrimination on an event-by-event basis by taking advantage of high speed signal  
91 sampling and digital signal processing. Therefore, data have been acquired with the  
92 experimental setup described in Section 2 to develop the approach of pile-up  
93 identification and reconstruction in NEDA. The principles and validation of the  
94 proposed approach are given and discussed in Section 3. The application of the  
95 approach in a high counting rate measurement is described in Section 4 and the  
96 conclusions in Section 5.

## 97 **2. Experiment**

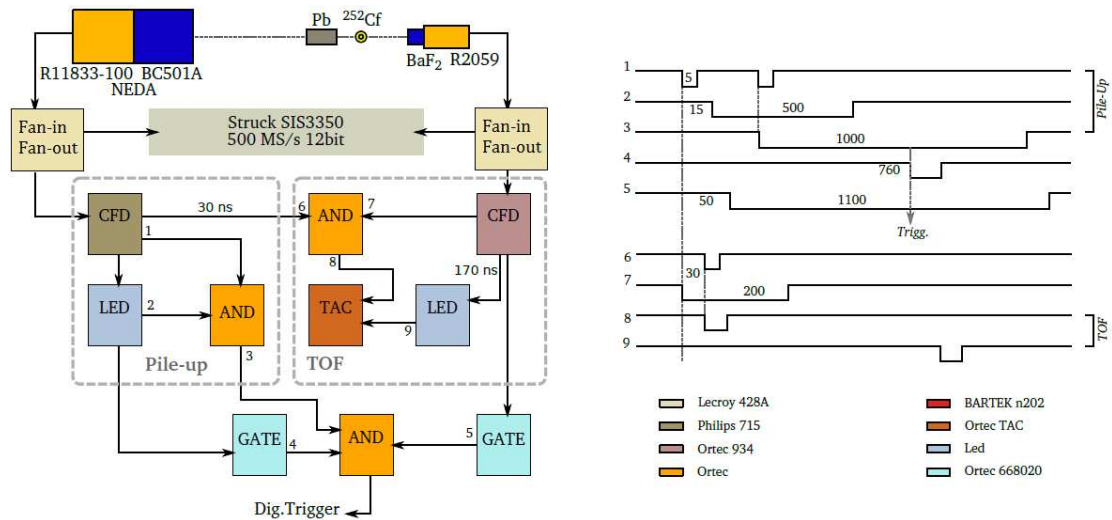
98 Two experiments were carried out at Laboratori Nazionali di Legnaro. The first  
99 was performed in order to acquire large numbers of single neutron or  $\gamma$  ray pulses,  
100 which were later used to extract standard neutron- and  $\gamma$ -induced pulses, and to  
101 generate synthetic pile-up pulses, aiming at developing the approach of pile-up  
102 identification and reconstruction in Section 3. The second experiment was performed  
103 in order to acquire large numbers of real pile-up pulses, which were later used to  
104 further evaluate the proposed method as shown in Section 4.

105 The experimental setup is illustrated in Fig. 1. The first experiment is almost the  
106 same as that of our previous work [10] except that only a single photomultiplier tube  
107 (PMT) of type Hamamatsu R11833-100 was used in this measurement. This 8-stage,  
108 5 in. diameter PMT, shielded with  $\mu$ -metal from magnetic fields, was coupled to a  
109 cylindrical 5 inch by 5 inch detector cell containing liquid scintillator of type  
110 BC-501A. The high voltage was set to get a signal amplitude of about 1 V/MeV using  
111 a  $^{60}\text{Co}$  source, which had an activity of about 2 MBq. A lead brick with a thickness of  
112 5 cm was put between the source and the BC-501A detector to reduce the counting  
113 rate originating from  $\gamma$  rays without losing too many neutrons, thus keeping the  
114 counting rate of the PMT R11833-100 at around 2 kHz. A trigger and time reference  
115 detector consisting of a cylindrical 1 inch by 1 inch  $\text{BaF}_2$  scintillator coupled to a 2  
116 inch R2059 PMT was placed very close to the  $^{252}\text{Cf}$  source for detection of  $\gamma$  rays.  
117 The threshold of the constant fraction discriminator (CFD) was set to approximately  
118 30 keVee (keV electron equivalent). With the outputs of the two CFD units fed into  
119 the LeCroy 465 coincidence unit, a coincidence between the signals from the  
120 BC-501A and  $\text{BaF}_2$  detectors was created, which was used as a trigger for the data  
121 acquisition system (GASIFIC) [15] and as a start signal for the time-to-amplitude  
122 converter (TAC). The counting rate of the  $\text{BaF}_2$  detector was about 200 kHz and the  
123 coincidence rate was about 200 Hz. The TAC module was subsequently stopped by  
124 the delayed signal from the  $\text{BaF}_2$  detector and measured the time-of-flight (TOF)  
125 difference between the detected  $\gamma$  rays and neutrons in the detectors. Signals from  
126 both detectors were digitised with a Struck SIS3350 digitiser [16] that has a 500 MHz  
127 sampling rate and 12-bit resolution (effective number of bits = 9.2). The analog TAC  
128 signals were digitised by a Struck SIS3302 digitiser working at a sampling rate of 100

129 MHz and with 16-bit resolution (effective number of bits  $\approx 13$ ).

130 In addition, a high count rate experiment was carried out by adding a pile-up  
 131 selector block to the first experimental setup (Fig. 1). In this measurement, the lead  
 132 brick was removed, and the distance between the BC-501A and the  $^{252}\text{Cf}$  source was  
 133 readjusted, which gave a count rate of 200 kHz in the BC-501A detector. Pile-up  
 134 events are validated by a logic AND (see signal 3 on the right), from the coincidence  
 135 of the NEDA CFD (signal 1) with the same signal delayed by 15 ns (to avoid  
 136 self-triggering) and wide open 500 ns (signal 2). To have the system triggered by the  
 137 first signal in the pile-up event, the CFD is further delayed with a gate delay generator  
 138 module (signal 4) and sent to another AND module in coincidence with signal 3. The  
 139 final trigger is then validated with a coincidence from the  $\text{BaF}_2$ . TOF is measured with  
 140 a TAC module, started with the coincidence (signal 8) of the two detector CFDs  
 141 (signals 6 and 7), triggered by the NEDA signal, and stopped with the  $\text{BaF}_2$  signal  
 142 delayed (signal 9). For the stop signal, a 170ns delay cable was used in order to  
 143 account for slow neutrons. As the logic signal is integrated through the cable, a  
 144 leading-edge discriminator (LED) was used afterwards to restore its step shape. The  
 145 trigger rate was about 200 Hz in this experiment. With this setup, pulses with intervals  
 146 ranging from 10 ns to 500 ns were recorded.

147 In this study, the digital signals from the BC-501A detector, as well as the TOF  
 148 information, were used for pile-up investigations.



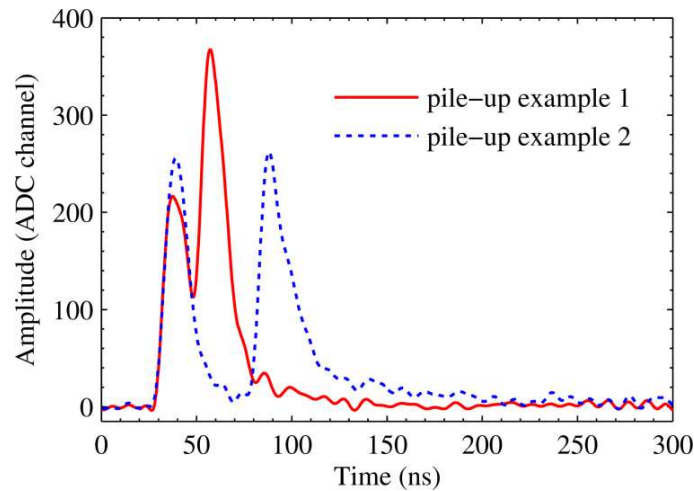
149  
 150 **Fig. 1.** Block scheme of the experimental setup (left) and the logic signals produced  
 151 (right).  
 152

### 153 3. Principles and validation of the approach

#### 154 3.1. Preprocessing of the signals

155 The 500 MHz sampling rate and 12-bit resolution of the Struck SIS3350 digitiser  
 156 allow detailed analysis and processing of the pulse waveforms from the BC-501A  
 157 detector, originating from either neutrons or  $\gamma$  rays. Fig. 2 gives two examples of  
 158 pile-up pulses after preprocessing, including CFD timing, baseline restoration and  
 159 filtering. For each waveform, a range of 300 ns of the pulse was used for the analysis,

160 as beyond this time span the first pulse has decayed to a negligible level [17], so that  
 161 the occurrence of a second pulse does not constitute a pile-up event. The start time of  
 162 the pulses constituting the pile-up event was determined by implementing a digital  
 163 CFD. The CFD method firstly attenuated the original signal to 20% of the first peak  
 164 amplitude, and then summed it with the delayed and inverted original signal. Finally,  
 165 the point that this sum signal crosses the zero axis was extracted, which is  
 166 independent of the pulse amplitude and corresponds to the time at which the original  
 167 pulse reaches 20% of its first peak amplitude. It can be seen in Fig. 2 that after the  
 168 CFD timing, the waveforms are well time aligned on the leading edge of the first peak.  
 169 Moreover, the baseline shift has been eliminated from each pulse by subtracting the  
 170 average value of the sampling points in the pre-trigger range of the waveform. A  
 171 small amount of severely distorted pulses with heavily fluctuating baselines have been  
 172 discarded (<1% of the total). In addition, a low-pass finite impulse response (FIR)  
 173 digital filter has been applied to the pulses to remove high-frequency noise [18].

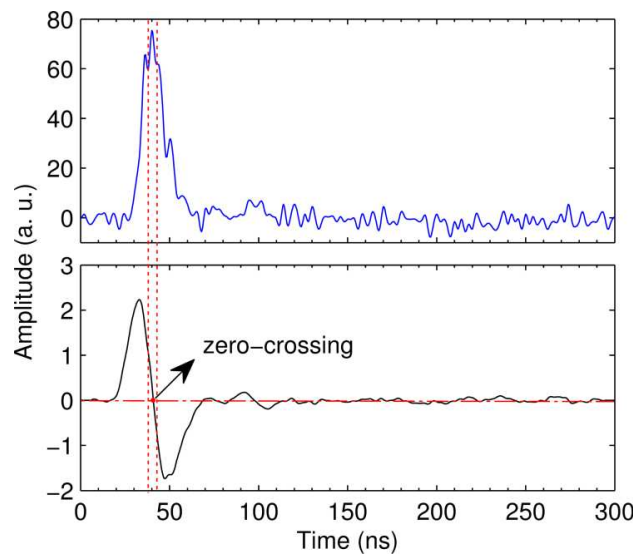


174  
 175 **Fig. 2.** Pile-up waveforms after the digital CFD time-aligning, baseline restoration, and filtering.  
 176

### 177 3.2. Pile-up pulse identification

178 When two or more peaks are detected within the duration of a recorded pulse  
 179 (300 ns in the present work), a pile-up event is identified. The common way of  
 180 detecting peaks is to search and find local maxima in the overlapping pulses, which  
 181 may misidentify the spikes in the waveforms as pile-up events. In particular, the low  
 182 energy signals are more likely to trigger false identifications because they are quite  
 183 noisy due to the scintillation statistics, and to the electronic noise and the quantisation  
 184 effects of the digitiser [19]. As shown in the upper plot of Fig. 3, the individual pulse  
 185 will be misinterpreted as a pile-up event by the maximum peak search method, as  
 186 more than two peaks can be detected. Therefore, another peak search method is  
 187 proposed here. It is based on the fact that the first-order derivative is the slope of the  
 188 original waveform and thus has a downward-going zero-crossing, which corresponds  
 189 to the peak maximum of the original waveform. Since the presence of spikes in the  
 190 original waveform will cause many false zero-crossings, the first-order derivative was  
 191 smoothed using a moving-average filter prior to searching for downward-going  
 192 zero-crossings [20]. Then, only those zero-crossings whose slope exceeds a certain

193 threshold at a point where the original signal exceeds a certain amplitude threshold  
 194 are counted. In this way the method detects only the desired peaks and ignores peaks  
 195 that are too small, too wide, or too narrow, which are mostly random noises. If two or  
 196 more peaks are detected in a signal, it is determined that a pile-up event has occurred.  
 197 It should be noted that the position of the peak is not exactly equivalent to the position  
 198 of the zero-crossing due to the fact that the smoothing can distort the waveform of the  
 199 first-order derivative slightly. The position and height of each peak are determined by  
 200 least-squares fitting of a segment of the original unsmoothed signal in the vicinity of  
 201 the zero-crossing. Fig. 3 shows an individual pulse and its first-order derivative to  
 202 illustrate the process of pile-up identification using the first-order derivative method,  
 203 in which the only one true peak is correctly detected.



204

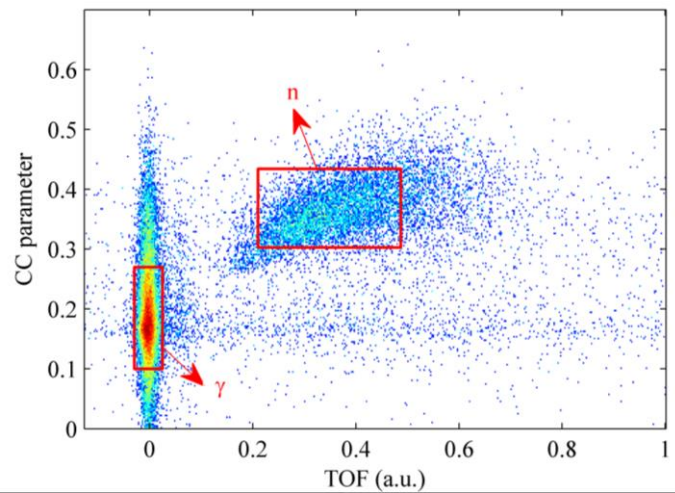
205 **Fig. 3.** An original waveform (upper panel) and its smoothed first-order derivative (lower panel).

206

### 207 3.3. Pile-up pulse reconstruction

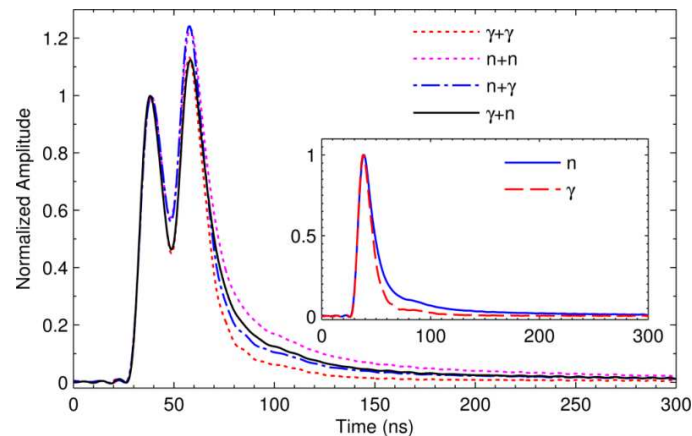
208 Once a pile-up event is identified using the first-order derivative method  
 209 described above, the next step is to resolve the overlapping pulses and reconstruct the  
 210 individual constituent pulses. Most of the existing pile-up resolving methods process  
 211 the first component and the second component of a pile-up event separately. The  
 212 fitting method, for instance, firstly recovers the first constituent pulse of a pile-up  
 213 event using a fitting procedure, and subsequently subtracts it from the original pile-up  
 214 pulse to obtain the second constituent pulse. In contrast, the approach proposed in this  
 215 paper treats the overlapping pulses that give rise to a pile-up event as a whole, which  
 216 is the combination of a single neutron or  $\gamma$  pulse. In this way there are only four  
 217 possible types of pile-up events under consideration, i.e.  $n+n$ ,  $\gamma+\gamma$ ,  $n+\gamma$ ,  $\gamma+n$ , which  
 218 means the combinations of the particle types of the first pulse and the second pulse.  
 219 The main principle of the approach is to build four corresponding models by  
 220 combining neutron and  $\gamma$  standard pulses with varying amplitude and time spacing,  
 221 which are then used to compare with the pile-up pulse, and the model that has the  
 222 highest degree of agreement with the pile-up pulse is determined as the type of the  
 223 pile-up event. The neutron and  $\gamma$ -ray standard pulses were obtained by averaging a

224 large number of neutron and  $\gamma$ -ray pulses respectively, which were extracted from n- $\gamma$   
 225 discrimination results of both the digital Charge Comparison (CC) [21] method and  
 226 the TOF measurement, as illustrated in Fig. 4. Although the TOF measurement is very  
 227 efficient to distinguish neutrons from  $\gamma$  rays, some misclassification cases still exist  
 228 due to accidental coincidences and to the emission of delayed  $\gamma$  rays from the  
 229 spontaneous fission of  $^{252}\text{Cf}$ . Therefore, the digital CC pulse shape discrimination  
 230 (PSD) method, based on comparing the integrated charge over two different time  
 231 periods of the pulse, was used to complement the TOF measurement to acquire as  
 232 pure neutron and gamma-ray pulses as possible. The CC parameter in Fig. 4  
 233 represents the ratio between the tail integral and the total integral, of which the start  
 234 points and end points have been optimised using the method of our previous work  
 235 [10].



236  
 237 **Fig. 4.** Density plot of the n- $\gamma$  discrimination parameter of the CC method versus the TOF of each pulse  
 238 recorded by the experimental equipment.

239  
 240 Figure 5 shows the normalized standard neutron- and  $\gamma$ -induced pulses, as well  
 241 as four pile-up models generated by adding pairs of standard pulses together separated  
 242 by a time interval of 20 ns. It can be seen that the pulse shapes of the resulting pile-up  
 243 models are quite distinguishable from each other, even though the constituent  
 244 standard pulses have normalized amplitudes and the same time intervals. Thus, these  
 245 differences in shape introduce the possibility of pile-up reconstruction based on the  
 246 four pile-up models.





248 **Fig. 5.** Four pile-up models generated by adding pairs of neutron or  $\gamma$  standard pulses (shown in the  
249 inset), which are separated by a time interval of 20 ns.

250

251 For an observed pile-up pulse waveform, two parameters can be easily estimated  
252 from its shape, i. e. the amplitude ratio  $A_r$  and time intervals  $T_i$  between the second  
253 peak and the first peak. The four pile-up models are constructed continuously until  
254 their  $A_r$  and  $T_i$  agree with those of the pile-up pulse using an iterative algorithm  
255 proceeding as follows:

256 (1) The  $A_r$  and  $T_i$  of the detected pile-up pulse are obtained with the first-order  
257 derivative method described in section 3.2.

258 (2) The pile-up pulse is normalized to the amplitude of its first peak.

259 (3) A standard pulse (neutron or  $\gamma$ ) is added with another standard pulse (neutron or  $\gamma$ )  
260 multiplied by  $k=(0.7+n)\cdot A_r$  (the initial value of  $n$  is set to 0) with the temporal  
261 separation of  $T_i$  to form four types of models.

262 (4) For each model, the sum pulse is normalized to the amplitude of its first peak, and  
263 then the amplitude ratio between the second peak and the first peak  $A_r'$ , which is  
264 the amplitude of the second peak after the normalization, is obtained.

265 (5) If  $A_r'$  is smaller/bigger than  $A_r$ , then  $n$  is increased/decreased by 0.001 and the  
266 process continues from step 3. If  $A_r'$  is equal to  $A_r$ , the iteration ends and the four  
267 models come to convergence.

268 Subsequently, the four models are evaluated point-by-point to the pile-up pulse  
269 that is normalized to the amplitude of its first peak respectively, and the model which  
270 has the minimum difference is determined as the type of the pile-up pulse  
271 ( $\gamma+\gamma/n+n/n+\gamma/\gamma+n$ ). In order to evaluate the difference, the factors of “minimum  
272 absolute value of the sum of point differences”, “minimum sum of absolute values of  
273 point differences”, “minimum sum of quadratic point differences”, and “minimum  
274 sum of quadratic relative point differences” were used respectively, it turned out that  
275 the method has the highest correct percentage when using the factor of “minimum  
276 absolute value of the sum of point differences”. The reason is that this factor takes  
277 into account plus-minus differences, while other factors make all differences positive.  
278 While in this case, the factor is used to evaluate the degree of fitting between the  
279 model and the pile-up pulse, so it's better to include both negative and positive  
280 differences. Therefore, the “minimum absolute value of the sum of point differences”  
281 is chosen as the factor to compare between the pile-up pulse and the models. After the  
282 model type is determined, the original constituent pulses giving rise to the pile-up  
283 event are reconstructed as the first standard pulse multiplied by  $A_1$  (amplitude of the  
284 first peak of the pile-up pulse) and the second standard pulse multiplied by  $k\cdot A_1$ .

285 For a proof of principle testing, synthetic pile-up data have been generated for  
286 four pile-up types respectively by randomly choosing pairs of single pulses of known  
287 types and adding them together with a controllable temporal separation, ranging from  
288 20 ns to 60 ns in steps of 4 ns. The dataset for each case consisted of 10,000  
289 synthesized pile-up pulses. The single pulses of known types were acquired by  
290 performing n- $\gamma$  discrimination with the combination of the CC method and the TOF  
291 measurement as shown in Fig. 4, with no extra threshold other than the CFD hardware

292 threshold of approximately 30 keVee. The dynamic range of these pulses, defined as  
 293 the ratio between the maximum and minimum amplitude pulses, was found to be  
 294 around 50. Four examples of the recovery of pile-up signals separated by 20 ns  
 295 between two peaks are given in Fig. 6, which shows the normalized pile-up pulses,  
 296 along with the corresponding models. It can be seen that the pile-up pulses all fit very  
 297 well with the corresponding models both on a linear scale, as well as on a logarithmic  
 298 scale shown in the insets. It is also clear from Fig. 6(a) that the other three models  
 299 except the  $\gamma+\gamma$  model are distinct from the pile-up pulse in shape, mainly in the tail  
 300 and the valley between the two peaks.

301

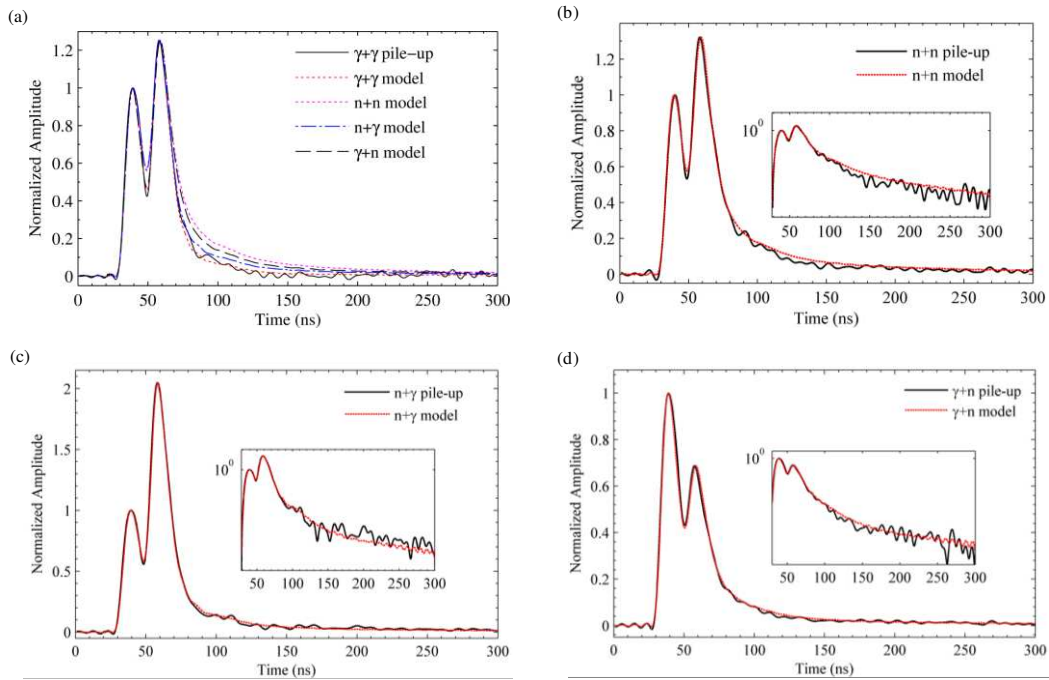
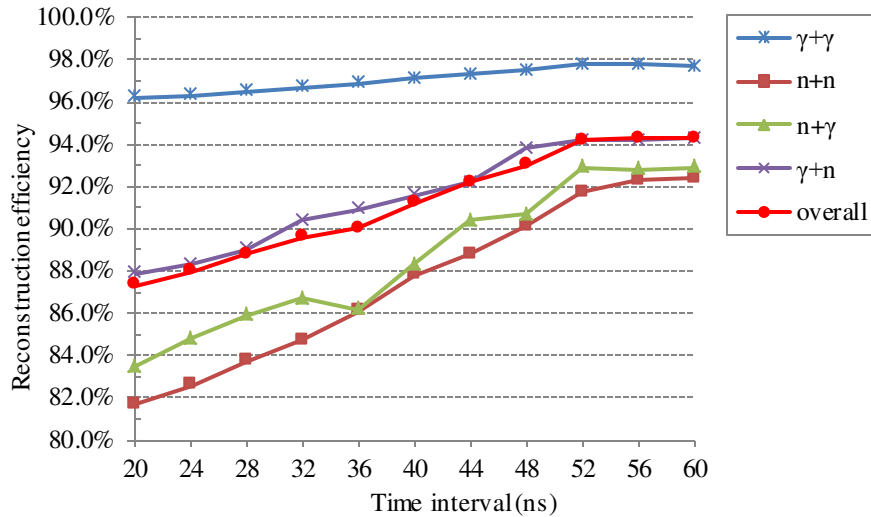


**Fig. 6.** Four types of pileup pulses which are separated by 20 ns and fitted with the corresponding models: (a)  $\gamma+\gamma$ , (b)  $n+n$ , (c)  $n+\gamma$ , and (d)  $\gamma+n$ .

306 Furthermore, the efficiency of the pile-up reconstruction method as a function of  
 307 the time interval between two pulses constituting a pile-up event has been investigated  
 308 using the synthetic pile-up data. Figure 7 illustrates the percentages of correctly  
 309 reconstructed pile-up events for each type with varying time intervals between two  
 310 constituent pulses, as well as the overall correct percentage for pile-up events  
 311 comprising of same counts of pulses belonging to the four pile-up types, which is  
 312 more realistic in practical nuclear experiments. It was found that a good performance  
 313 in resolving pile-up events can be obtained from a time interval of 20 ns onwards. The  
 314 overall correct percentage is around 90% with time intervals from 20 ns to 48 ns,  
 315 while the error of reconstructing pile-up events can be kept below 6% when  
 316 successive peaks are separated by more than 50 ns. It should be noted that this method  
 317 almost failed to reconstruct pile-up pulses with time intervals below 20 ns, as the  
 318 reconstructing accuracy deteriorated sharply from 20 ns downwards.



320 **Fig. 7.** The percentages of correctly reconstructed pile-up events versus the separation time between the  
 321 two constituent pulses.

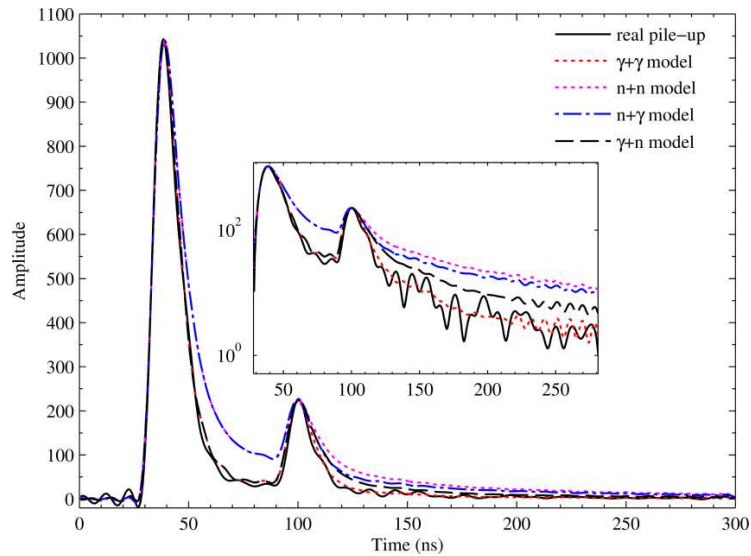
322 The results also indicate that the efficiency of the pile-up identification and  
 323 reconstruction method depends on the type of pile-up pulses, and the time interval  
 324 between the two constituent pulses. In general, the correctly reconstructed fractions of  
 325 all types of the pile-up events improve as the time intervals increase. Meanwhile, the  
 326 performance of the method varies among different types of pile-up events, while the  
 327 type of  $\gamma+\gamma$  has the highest efficiency. This is reasonable as the pulse width of the  
 328 standard  $\gamma$ -ray pulse is relatively narrow compared with that of the standard neutron  
 329 pulse, thereby leading to less information lost in a pile-up pulse with a certain time  
 330 interval between two peaks. For each case there are always some mistakenly  
 331 reconstructed pile-up events that are caused by two reasons. One is the intrinsic  
 332 limitation of the method when dealing with extreme cases, in which the pulse  
 333 amplitude ratio is too large or the pulse temporal separation is too small. The other  
 334 one is the type of pulses that are used for generating synthetic pile-up data sets can  
 335 contain some misinterpreted neutron-gamma events, even though both the CC method  
 336 and the TOF measurement were combined to discriminate them. Therefore, some  
 337 correct reconstruction cases could be misclassified as wrong cases, as the pre-known  
 338 types of the constituent pulses are in themselves wrong. However, the large  
 339 percentages of correctly reconstructed pile-up events has demonstrated the  
 340 effectiveness of this method, allowing it to be used for correcting the spectra distorted  
 341 by pile-up events as shown in next section.

#### 342 **4. Application of the new method to NEDA data**

343 In order to further evaluate the performance of the pulse pile-up identification  
 344 and reconstruction method presented, it has been applied to the pile-up events from  
 345 the high count-rate measurement described in Section 2.

346 By applying the approach of pulse pile-up identification and reconstruction to the  
 347 experimental data, 66916 pile-up events have been detected in a total of 92239 events,  
 348 which account for approximately 72.5% of the total events. It was empirically found

349 that the method was able to locate the positions and to measure the amplitudes of the  
 350 peaks in the pile-up events automatically and reconstruct them accurately, even  
 351 though the peaks were randomly spaced in time and vary in amplitude. It should be  
 352 noted that reconstruction processing here was restricted to the pile-up pulses arising  
 353 from two events. Figure 8 shows an example of real pile-up identification and  
 354 reconstruction. Despite the large pulse amplitude ratio between the two peaks, the  
 355 result of resolving the pile-up event is quite satisfactory.

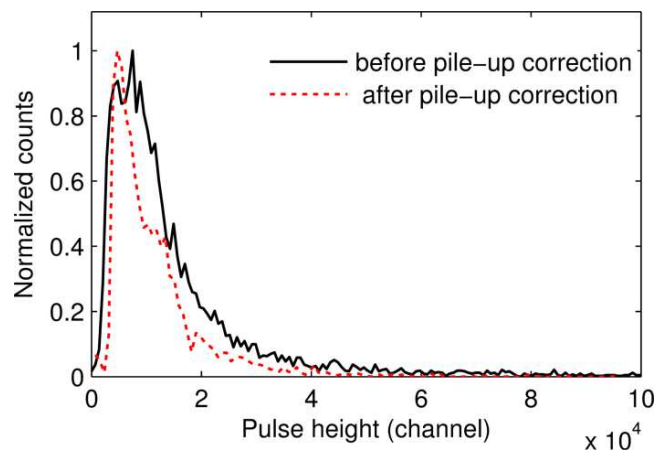


356

357 **Fig. 8.** A case of pile-up identification and reconstruction in the high counting rate measurement.

358

359 Rather than discarding the pile-up pulses, the new method can now allow them to  
 360 be included in spectral analysis. Figure 9 shows the neutron pulse height spectra of  
 361  $^{252}\text{Cf}$  before and after the pile-up correction, obtained by summing sampling points  
 362 over the whole pulse width. Severe spectral distortions can be seen in the pulse height  
 363 spectrum of the signals without pile-up correction. These distortions owing to pile-up  
 364 events have been corrected significantly after applying the pulse pile-up identification  
 365 and reconstruction method.



366

367 **Fig. 9.** The neutron pulse height spectra of  $^{252}\text{Cf}$  before and after the pile-up correction (66916 pile-up  
 368 events have been detected and reconstructed in a total of 92239 events).

369

## 370 **5. Conclusions**

371 A new method designed to deal with digital pulse pile-up identification and pulse  
372 reconstruction is presented in this paper. The digitised waveforms used for developing  
373 and validating the method were acquired with an experimental setup consisting of a  
374  $^{252}\text{Cf}$  source, a BC-501A detector and a SIS3530 digitiser with a sampling rate of 500  
375 MHz and with 12-bit resolution. When identifying pile-up events by searching for the  
376 downward-going zero-crossings in the smoothed first-order derivative of the original  
377 pulse, the method was less vulnerable to fluctuations in the signal compared with the  
378 conventional maximum peak search method. Moreover, rather than discarding the  
379 detected pile-up pulses, as is the case in hardware-based pile-up rejectors, this method  
380 allows the reconstruction of the individual components of the pile-up events  
381 employing four models that are generated by combining pairs of neutron and  $\gamma$   
382 standard pulses. Tests performed both on synthetic and experimental data  
383 demonstrated that the method was capable of recovering two overlapping signals with  
384 a high accuracy even when they are spaced in time as close as 20 ns. However, it  
385 should be noted that the method can only be applied to pile-up events where two  
386 pulses overlap. Since this method can provide reliable information of the constituent  
387 particles of the pile-up events, thus avoiding losses of counting statistics and  
388 distortions of pulse height spectra, it is of practical use to eliminate pulse pile-up  
389 effects on the neutron-gamma discrimination performance of liquid scintillator  
390 detectors used at high count rates.

## 391 **Acknowledgments**

392 This work was partly funded by the Swedish Research Council, by the UK STFC,  
393 under grant ST/L005727/1, by the Generalitat Valenciana, Spain, under grant  
394 PROMETEO/2010/101, by MINECO, Spain, under grants AIC-D-2011-0746,  
395 FPA2011-29854 and FPA2012-33650, and by TUBITAK, Turkey, under grant  
396 114F473.

397

## 398 **References**

- 399 [1] J. Bartosek, J. Masek, F. Adams, J. Hosle, Nuclear Instruments and Methods in Physics Research  
400 104 (1972) 221.
- 401 [2] R.P. Gardner, L. Wielopolski, Nuclear Instruments and Methods in Physics Research 140 (1977)  
402 289.
- 403 [3] D.W. Datlowe, Nuclear Instruments and Methods in Physics Research 145 (1977) 379.
- 404 [4] P.C. Johns, M.J. Yaffe, Nuclear Instruments and Methods in Physics Research Section A 255 (1981)  
405 559.
- 406 [5] G.F. Knoll, Radiation Detection and Measurement, fourth ed., Wiley, New York, 2010.
- 407 [6] S. Marrone, D. Cano-Ott, N. Colonna, et al., Nuclear Instruments and Methods in Physics Research  
408 Section A 490 (2002) 299.
- 409 [7] F. Belli, B. Esposito, D. Marocco, et al., Nuclear Instruments and Methods in Physics Research  
410 Section A 595 (2008) 512.

- 411 [8] W. Guo, R.P. Gardner, C. W. Mayo, Nuclear Instruments and Methods in Physics Research Section  
412 A 544 (2005) 668.
- 413 [9] G. Jaworski, M. Palacz, J. Nyberg, et al., Nuclear Instruments and Methods in Physics Res earch  
414 Section A 673 (2012) 64.
- 415 [10] X.L. Luo, V. Modamio, J. Nyberg, J.J. Valiente-Dobón, et al., Nuclear Instruments and Methods in  
416 Physics Research Section A 767 (2014) 83.
- 417 [11] F.J. Egea, C. Houarner, A. Boujrad, et al., IEEE transactions on nuclear science 62 (2015)1063.
- 418 [12] V. Modamio, J.J. Valiente-Dobón, et al., Nuclear Instruments and Methods in Physics Research  
419 Section A 775 (2015) 71.
- 420 [13] J.J. Valiente-Dobon et al., Nuclear Instruments and Methods in Physics Research Section A (to be  
421 submitted).
- 422 [14] A. Gadea, E. Farnea, J.J. Valiente-Dobón, et al., Nuclear Instruments and Methods in Physics  
423 Research Section A 654 (2011) 88.
- 424 [15] S. Akkoyun, A. Algora, B. Alikhani, et al., Nuclear Instruments and Methods in Physics Research  
425 Section A 668 (2012) 26.
- 426 [16] J. Agramunt, J. L. Tain, et al., Nuclear Instruments and Methods in Physics Research Section A  
427 807 (2016) 69.
- 428 [17] <<http://www.struck.de/sis3350.htm>>2014.
- 429 [18] M. Moszyński, G.J. Costa, G. Guillaume, et al., Nuclear Instruments and Methods in Physics  
430 Research Section A 350 (1994) 226.
- 431 [19] A.V. Oppenheim, Signals and Systems, second ed., Pearson, New Jersey, 1996.
- 432 [20] X.L. Luo, Y.K. Wang, G. Liu, J. Yang, et al., Nuclear Instruments and Methods in Physics  
433 Research Section A 717 (2013) 44.
- 434 [21] G.R. Arce, Nonlinear Signal Processing: A Statistical Approach, Willy, New Jersey, 2005.
- 435 [22] F.D. Brooks, Nuclear Instruments and Methods in Physics Research Section 4 (1959) 151.